Pharmacodynamic evaluation of plasma and epithelial lining fluid exposures of amikacin against *Pseudomonas aeruginosa* in a dynamic *in vitro* hollow-fibre infection model.

Aaron J. Heffernan [a,b,#], Fekade B. Sime [b,c], Derek S. Sarovich [d], Michael Neely [e], Yarmarly Guerra-Valero [c], Saiyuri Naicker [b,c], Kyra Cottrell [c], Patrick Harris [c,f], Katherine T. Andrews [g], David Ellwood [a,h], Steven C. Wallis [c], Jeffrey Lipman [c,i,j], Keith Grimwood [a,k], Jason A. Roberts [b,c,i,j]

a School of Medicine, Griffith University, Gold Coast, Queensland 4222, Australia

b Centre for Translational Anti-Infective Pharmacodynamics, School of Pharmacy, The University of Queensland, Brisbane, Queensland 4102, Australia

c University of Queensland Centre for Clinical Research, Faculty of Medicine, The University of Queensland, Brisbane, Queensland 4029, Australia

d GeneCology Research Centre, University of the Sunshine Coast, Sippy Downs, Queensland 4556, Australia

e Children's Hospital Los Angeles, University of Southern California Keck School of Medicine, Los Angeles, California, United States of America

f Department of Microbiology, Pathology Queensland, Royal Brisbane and Women's Hospital, Brisbane, Queensland, Australia

g Griffith Institute for Drug Discovery, Griffith University, Nathan, Queensland 4111, Australia

h Department of Maternal and Fetal Medicine, Gold Coast Health, Southport, Queensland 4215, Australia

i Department of Intensive Care Medicine, Royal Brisbane and Women's Hospital, Brisbane, Queensland 4029, Australia

j Division of Anaesthesiology Critical Care Emergency and Pain Medicine, Nîmes University Hospital, University of Montpellier, Nîmes France

k Department of Paediatrics, Gold Coast Health, Southport, Queensland 4215, Australia

Running Title: Pharmacodynamics of intravenous amikacin

Corresponding author #: Mr Aaron Heffernan

Centre for Translational Anti-Infective Pharmacodynamics, School of Pharmacy, The University of Queensland, Cornwall St, Buranda, Queensland 4102, Australia

Ph +61 7 3346 1814 Fax +61 7 3646 3542

E-mail- aaron.heffernan@griffithuni.edu.au

Abstract

Given that aminoglycosides, such as amikacin, may be used for multi-drug resistant *Pseudomonas aeruginosa* infections, optimization of therapy is paramount for improved treatment outcomes. This study aims to investigate the pharmacodynamics of different simulated intravenous amikacin doses on susceptible *P. aeruginosa* to inform ventilator-associated pneumonia and sepsis treatment choices.

A hollow-fibre infection model with two *P. aeruginosa* isolates (MIC 2 and 8 mg/L) with an initial inoculum ~10^8 colony-forming unit/mL was used to test different amikacin dosing regimens. Three regimens (15, 25 and 50 mg/kg) simulating a blood exposure and a 30 mg/kg regimen simulating the epithelial lining fluid (ELF) for potential respiratory tract infection were tested. Data were described using a semi-mechanistic pharmacokinetic/pharmacodynamic (PK/PD) model. Whole genome sequencing was used to identify mutations associated with resistance emergence.

While bacterial density was reduced by >6-logs within the first 12 h in simulated blood exposures, following this initial bacterial kill, there was amplification of a resistant sub-population with ribosomal mutations that were likely mediating amikacin resistance. No appreciable bacterial killing occurred with subsequent doses. There was less (<5-log) bacterial killing in the simulated ELF exposure for either isolate tested. Simulation studies suggest that a dose of 30 and 50 mg/kg may provide maximal bacterial killing for bloodstream and VAP infections respectively.

Our results suggest that amikacin efficacy may be improved with the use of high dose therapy to rapidly eliminate susceptible bacteria. Subsequent doses may have reduced efficacy given the rapid amplification of less-susceptible bacterial subpopulations with amikacin monotherapy.

Introduction

Sepsis or ventilator-associated pneumonia (VAP) caused by *Pseudomonas aeruginosa* is associated with a mortality of between 25 and 50% (1, 2). Furthermore, patients with carbapenem-resistant *P. aeruginosa* infections have an increased risk of death that may be attributed to increasing illness severity, and delayed administration of appropriate antibiotic therapy (3-6). Despite a potential increased mortality with aminoglycoside monotherapy, at least 80% of *P. aeruginosa* isolates remain susceptible to aminoglycosides such as amikacin, therefore they may be prescribed for empiric treatment as part of combination therapy to appropriately extend the spectrum of antibiotic activity in settings with increased resistance rates (3-6).

One potential contributing factor to the apparent reduced efficacy of aminoglycosides is suboptimal dosing. Achieving an aminoglycoside maximum concentration (C_{max}) to minimum inhibitory concentration (MIC) ratio ≥10 or an area under the-concentration time-curve (AUC) to MIC ratio ≥150 reduces mortality and hastens symptom resolution (7, 8) Importantly, the risk of resistance emergence and potential treatment failure may be increased when bacteria are exposed to a C_{max}/MIC <6 (9). Moreover, in patients infected with carbapenem-resistant, aminoglycoside-susceptible *Klebsiella pneumoniae*, aminoglycosides have been associated with favourable outcomes, particularly when a therapeutic aminoglycoside exposure may be possible at the site of infection (bloodstream, vascular catheters, soft tissues, and urinary tract) (10).

Aminoglycoside dose optimization must also consider the potential effect of the bacterial inoculum, the immune response, and the potential toxicity of the dosing regimen. Approximately one-third of patients with VAP have a bacterial burden exceeding 10^8 colony forming units (CFU)/mL (11, 12). Reducing this bacterial burden to <$1x10^6$ CFU/mL may

enable rapid granulocyte mediated bacterial clearance and enhance symptom resolution (11-13). These factors may be particularly important in patients with Gram-negative bacillary pneumonia for two reasons. First, amikacin penetration into the epithelial lining fluid (ELF), the site of infection, is only approximately 10% of the plasma C_{max} (14). Second, there may be limited treatment options available for multi-drug resistant bacteria should aminoglycoside therapy fail.

The aims of this study were twofold. First, to describe and quantify the time course of bacterial killing and emergence of resistance of two *P. aeruginosa* clinical isolates using the dynamic *in vitro* hollow-fibre infection model (HFIM) and semi-mechanistic mathematical modelling. Second, to determine amikacin dosing regimens that may enhance bacterial killing in both the bloodstream and ELF.

Materials and Methods

Antimicrobial agents

Amikacin analytical reference standards (Sigma-Aldrich, batch number LRAA5755) were used for *in vitro* MIC susceptibility testing and preparing amikacin-containing cation adjusted Mueller-Hinton (Ca-MH) agar plates. Commercially available amikacin vials (DBL Amikacin sulphate 500mg/2mL, batch number CO61221AA) stored at 4°C were used for HFIM dosing. Amikacin stock solutions were aseptically prepared in a Class II biosafety cabinet by diluting amikacin with sterile distilled water and storing at -80°C.

Bacterial isolates

Two clinical *P. aeruginosa* isolates (#CTAP40 and #CTAP23) were sourced from critically ill patients. Isolates were stored in Ca-MH broth with 20% glycerol v/v at -80 ℃ and were grown on Ca-MH agar and incubated at 37 ℃ for 24 h prior to *in vitro* susceptibility testing and HFIM studies. A 0.5 McFarland bacterial suspension was prepared in sterile water using morphologically similar colonies and diluted in Ca-MH broth to the desired inoculum. For HFIM studies, bacteria were suspended in 40 mL of Ca-MH broth and incubated at 37 ℃ with constant agitation for a duration of time based on previous growth curves to achieve a final inoculum of approximately 10^8 CFU/mL.

In vitro susceptibility testing

Broth microdilution was performed in accordance with Clinical & Laboratory Standards Institute (CLSI) and the European Committee on Antimicrobial Susceptibility Testing (EUCAST) guidelines (15, 16). Briefly, a volume of bacteria suspended in Ca-MH broth (final inoculum $5.5x10^5$ CFU/mL) was added to a 96-well flat or round bottom plate containing serial twofold dilutions of amikacin in Ca-MH broth. Inoculated 96-well plates were incubated for 16-24 h at 37 ℃. Round bottom plates were visually inspected for growth; the lowest amikacin concentration with no apparent growth was defined as the MIC. The MIC for the flat bottom plates was determined using a Multiskan FC Microplate Photometer (Thermo Fisher Scientific, Finland), and defined as the concentration with an optical density <0.1 of the growth control. The modal MIC of four replicates within an individual experiment for each method (CLSI and EUCAST) was selected as the isolate MIC.

Mutation frequency

A 10 mL culture of a 10^2 CFU/mL inoculum was incubated in Ca-MH broth for 24 h at 37°C. Quantitative culturing methods with diluted and undiluted samples were performed on the resultant bacterial growth using both standard Ca-MH agar and amikacin-containing Ca-MH agar (fourfold baseline MIC). The mutation frequency was taken as the ratio of the bacterial concentration growing on amikacin-containing plates to the initial inoculum after incubating for 48 h at 37°C.

Hollow-Fibre Infection Model

The HFIM was assembled as described previously using FiberCell Systems polysulfone cartridges (C2011) in all experiments and conducted over 7 days (17, 18). One HFIM experiment was conducted for each dosing regimen and isolate combination with an initial bacterial concentration of $1x10^8$ CFU/mL.

Unbound amikacin blood exposures were simulated using the pharmacokinetic model derived by Romano et al., assuming an 80 kg patient with sepsis, a creatinine clearance of 100 mL/min, and 17% protein binding (19, 20). Amikacin dosing regimens of 15, 25, and 50 mg/kg once-daily infused over 30-minutes were tested. High 50 mg/kg doses were also tested given that these doses have been previously used clinically (21). The ELF amikacin concentrations and resultant half-life in the HFIM apparatus were approximated using previous aminoglycoside ELF:serum ratios in conjunction with the established concentration-time curves for the blood amikacin exposure (14, 22, 23). In brief, the estimated unbound plasma concentration of amikacin was multiplied by the average ELF:serum penetration ratio (0.12, 0.3, 0.85, 1.14) identified for other aminoglycosides (gentamicin and tobramycin) at

171 the corresponding time points (0.5, 1, 2, 4 h) (14, 22, 23). The ELF half-life (1.92 h) was
172 derived from a non-compartmental analysis of the resultant concentration-time curve over the
173 course of 24 h, which approximates that identified previously (24, 25). A mucin bound
174 fraction of 50% was assumed, representing a likely worst-case scenario (26). An ELF
175 amikacin exposure following an intravenous dose of 30 mg/kg once-daily administered over
176 30-minutes was simulated.

177

178 Samples were periodically removed from the central compartment outlet at 0.25, 0.5, 0.45, 1,
179 2, 3, 4, 6, 8, 10, 12, 24, 25, 30, 36, 48, 49, 54, 60, 72, 73, 78, 84, 96, 120, 144, 145, and 156 h
180 to determine the amikacin concentration for pharmacokinetic analysis. As the central
181 compartment contents rapidly equilibrate with the hollow-fibre cartridge, the concentrations
182 obtained in the central compartment reflect that in the hollow-fibre cartridge. Bacterial
183 quantification was performed with periodic sampling at 0, 2, 4, 6, 8, 11, 24, 35, 48, 59, 72,
184 96, 120, 144 and up to 168 h from the cartridge extra-capillary space. Samples were washed
185 twice in phosphate-buffered saline to minimise antibiotic carry-over. A 100 µL aliquot of an
186 appropriately diluted bacterial suspension was manually plated onto Ca-MH agar and
187 amikacin-containing Ca-MH agar (fourfold baseline isolate MIC). The limit of quantification
188 was 2-$\log_{10}$ CFU/mL.

189

190 *Drug assay*

191 Amikacin was measured in Ca-MH broth by a validated Liquid Chromatography Mass
192 Spectrometry method. Briefly, 50 µL of Ca-MH broth sample (neat or diluted) was combined
193 with 50 µL of water and 20 µL of vancomycin (50 mg/L) added as the internal standard.
194 Amikacin was extracted using protein precipitation with 50 µL of trichloroacetic acid (15%,

v/v). Samples were centrifuged at 12,000 g for 5-minutes and an aliquot of the supernatant (0.5 µL) was injected onto a Nexera2 UHPLC system coupled to an 8030+ triple quadrupole MS detector (Shimadzu, Kyoto, Japan). Chromatographic separation was achieved using a Poroshell 120 HILIC column (Agilent, Santa Clara, USA) and a gradient of formic acid 0.2% v/v and acetonitrile with 0.2% formic acid v/v. Detection of amikacin and the internal standard was performed using an electrospray source in positive mode with optimised multiple reaction monitoring conditions for each analyte. Amikacin was monitored at three fragmentation ions (586.25 → 163.10, 586.25 → 264.15 and 586.25 → 425.15) and vancomycin was monitored at two fragmentation ions (725.60 →144.10 and 746.10 → 144.20).

Calibration lines of amikacin were quadratic with 1/concentration^2 weighting from 0.2 to 10 mg/L with a maximum deviation from the nominal concentration of 2.1%. Mean intra-batch accuracy and precision values were -6.2% and 8.3% at 0.8 and 8 mg/L respectively.

Whole Genome Sequencing

Bacterial isolates for whole genome sequencing were subcultured onto amikacin-containing (4x baseline MIC) CaMH agar as the resistant bacterial population profile may be transient without the presence of amikacin. Bacterial DNA was extracted without single colony purification to capture population diversity using the DNeasy UltraClean DNA Extraction in accordance with the manufacturer's directions and quantified using spectrophotometry (NanoDrop; ThermoFisher) and fluorometry (Qubit; ThermoFisher). Paired-end DNA libraries were prepared using the Nextera kit (Illumina; Australia) in accordance with the manufacturer's directions. Sequencing was performed using the Illumina Mini-Seq (150 bp paired ends). Improved draft genome assemblies were constructed for the two progenitor

strains, #CTAP23 and #CTAP40, using the Microbial Genome Assembler Pipeline (MGAP v1.1)27, and annotated using Prokka v1.12.28 The comparative genomics pipeline, SPANDx29 v3.2.1, was used to determine genomic variation using the either the #CTAP23 or #CTAP40 as the reference genome depending on the lineage analysed. Within species mixtures were analysed using the GATK v4.1.0.030 to identify mutations with less than 100% allele frequency using the method outlined in Aziz et al. (31).

Mathematical Pharmacokinetic/Pharmacodynamic Modelling

All HFIM data from simulated bloodstream exposures were co-modelled using Pmetrics for R version 1.5.2 considering the results of the whole genome sequencing study (32, 33). The final structural model is described by equations 1 to 5 that describe amikacin pharmacokinetics and bacterial growth of three subpopulations. Model diagnostics including the Akaike-information-criteria, log-likelihood, coefficient of determination (R^2) from the observed vs. expected plots, and visual-predictive-checks were used to evaluate and compare models.

Equation 1:

$$\frac{dAmk}{dt} = R(1) - \left(\frac{CL}{Vc} \times Amk\right)$$

Equation 2:

$$\frac{dCFUs}{dt} = K_{gmax,s} \times CFU_s \times \left(\frac{Qmax \times Sub}{Qs + Sub}\right) - CFU_s \times K_{killmax,s} \times \left(\frac{\frac{Amk^{Hs}}{Vc}}{EC50_s^{Hs} + \frac{Amk^{Hs}}{Vc}}\right) - Kds \times CFU_s$$

Antimicrobial Agents and Chemotherapy

Equation 3:

$$\frac{dCFUi}{dt} = K_{gmax,i} \times CFU_i \times \left(\frac{Qmax \times Sub}{Qs + Sub}\right) - CFU_i \times K_{killmax,i} \times \left(\frac{\frac{Amk^{Hi}}{Vc}}{EC50_i^{Hi} + \frac{Amk^{Hi}}{Vc}}\right) - Kdi \times CFU_i$$

Equation 4:

$$\frac{dCFUr}{dt} = K_{gmax,r} \times CFU_r \times \left(\frac{Qmax \times Sub}{Qs + Sub}\right) - Kdr \times CFU_r$$

Equation 5:

$$\frac{dSub}{dt} = -\left(\frac{Qmax \times Sub}{Qs + Sub}\right) \times (CFU_s + CFU_i + CFU_r)$$

Equation 1 describes amikacin elimination. Equations 2, 3, and 4 describe the bacterial growth, including the theoretical maximal bacterial density and amikacin-mediated killing of the susceptible, intermediate and resistant bacterial populations respectively. Equation 5 describes the consumption of an artificial substrate (Sub) required for sustained bacterial growth.

Amk amount of amikacin (mg); R(1) amikacin infusion rate (mg/h); CL amikacin clearance; Vc HFIM circuit volume; CFUs, CFUi, and CFUr representing the bacterial burden for the susceptible, intermediate, and resistant *P. aeruginosa* subpopulations respectively (CFU/mL); Kgmax,s, Kgmax,I, Kgmax,r maximal growth rate constants for the susceptible, intermediate, and resistant *P. aeruginosa* subpopulations respectively (log_{10} CFU/mL/h); Kkillmax,s, Kkillmax,i are the maximum rate of amikacin-mediated bacterial killing (log_{10} CFU/mL/h);

Kds, Kdi and Kdr intrinsic bacterial death rate constants for the susceptible, intermediate and resistant subpopulations (log_{10} CFU/mL/h); EC50s and EC50i amikacin concentration producing half-maximal bacterial killing for the susceptible and intermediate subpopulations respectively; Sub amount of a fictitious substance required for bacterial growth; Qmax maximum rate of substance use; Qs 50% of maximal substance use; Hs and Hi slope functions for the susceptible and intermediate subpopulations respectively.

Monte Carlo dosing simulation studies (n=1000) were performed using Pmetrics. Mean pharmacokinetic parameter estimates, as well as standard deviations of the clearance and volume of distribution, were obtained from the study conducted by Romano et al. (19) and applied to the simulations for the pharmacodynamic model. Mean value pharmacodynamic model parameters were estimated for specific isolates and were used for simulations. Moreover, different creatinine clearance values were used to describe patients with lower, normal and high renal amikacin clearance. The *f*AUC within the first 24 h was calculated employing Pmetrics, which included both the period of infusion and the monoexponential decay. Classification and regression tree analyses (CART) were used to determine the amikacin *f*AUC (mg.h/L) achieving stasis, 1-log, and 2-log reduction in the bacterial concentration within the first 24 h.

Results

In vitro susceptibility and mutational frequency studies

The modal amikacin MIC for #CTAP23 and #CTAP40 was 2 and 8 mg/L respectively. The mutation frequency for #CTAP23 and #CTAP40 in the presence of 8 and 32 mg/L of amikacin was 6.77×10^{-7} and 1.05×10^{-7} respectively.

Hollow-Fibre Infection Model

All intravenous amikacin dosing regimens against a simulated bloodstream *P. aeruginosa* infection resulted in a ≥4-log reduction from the starting inoculum (10^8 CFU/mL) during the first 8 h following the first dose of amikacin (Figure 1). There was no appreciable difference in the rate or extent of bacterial killing between the 15, 25 and 50 mg/kg dosing regimens for #CTAP23 (MIC 2 mg/L) (Figure 1, A). However, there was an approximate 1.5-log difference in the bacterial nadir between the 25 mg/kg and 50 mg/kg dosing regimens against #CTAP 40 (MIC 8 mg/L) (Figure 1, B). The total bacterial burden surpassed the baseline inoculum by 24 h for both isolates following administration of the 15 and 25 mg/kg dosing regimens. Only the 50 mg/kg dosing regimen for both isolates delayed the rate of bacterial regrowth, exceeding the baseline inoculum by 48 h (Figure 1). Bacterial regrowth in the total population was mirrored by bacterial growth on amikacin-containing CaMH agar (Figure 2). The MIC of the bacteria growing on amikacin-containing CaMH agar increased by a minimum of eightfold after seven days of amikacin administration for both isolates tested (Table 1).

A similar pattern was observed against the simulated ELF exposure. The total bacterial population was reduced by approximately 5-logs, 8 h after the initiation of the amikacin against #CTAP23 (MIC 2 mg/L), which was followed by rapid bacterial regrowth exceeding the baseline inoculum by 24 h, mirrored by growth on amikacin-containing CAMH agar

(Figure 1, A; Figure 2). Conversely, there was little appreciable bacterial killing against #CTAP40 (MIC 8 mg/L), yet there was an increase in the growth on amikacin-containing CaMH agar (Figure 2). There was no appreciable bacterial killing following subsequent dosing events after day 1 of amikacin in either the blood or ELF exposures in the HFIM. The observed amikacin concentrations for the simulated unbound plasma and ELF approximated the expected concentrations (Graph A in Figures 3 and 4).

Comparative genomic analysis

There were no resistance genes or single nucleotide polymorphisms (SNPs) associated with amikacin resistance identified in the progenitor strains, #CTAP23 or #CTAP40, prior to amikacin commencement. *De novo* SNPs within the *fusA (*$FusA_{Leu464Val}$) and *rplB* ($RplB_{Gly138Leu}$) genes were identified in isolates that were exposed to the 25 and 50 mg/kg daily dosing regimens respectively for #CTAP23 (Table 2). No SNPs were identified following exposure to amikacin 15 mg/kg. SNPs were identified in the *algA* and *tuf1* ($Tuf1_{Val21Leu}$) genes for #CTAP40 following exposure to amikacin; with a small baseline bacterial subpopulation containing an *algA* ($AlgA_{Ala279Asp}$) SNP.

Pharmacokinetic/Pharmacodynamic Modelling

Pharmacodynamic parameter estimates are detailed in Table 3. The average total bacterial population Bayesian posterior (model fitted estimate for each individual experimental arm) correlation coefficient (R^2) was 0.97 and 0.78 for #CTAP23 (Figure 3) and #CTAP40 (Figure 4) simulated blood exposures respectively. Similar results were found for the resistant bacterial population (average Bayesian posterior R^2 0.97 and 0.95 for #CTAP23 and #CTAP40 respectively).

CART analysis identified similar *f*AUC and fC_{max} thresholds for bacterial stasis for both isolates over 24 h; correlating with a difference in the *f*AUC/MIC and the fC_{max}/MIC ratio relative to the isolate MIC (Table 4). However, no threshold was associated with a bacterial kill in the bloodstream of 1- or 2-logs over 24 h for #CTAP23. Amikacin simulated *f*AUC and fC_{max} ELF exposures were increased relative to plasma for the same bacterial kill over 24 h and was increased for #CTAP23 (MIC 2 mg/L) compared with #CTAP40 (MIC 8 mg/L). The probability of achieving bacterial stasis, 1- and 2-log kill after 24 h is generally high in the ELF and the bloodstream when doses ≥30 mg/kg are used (Table 5).

Discussion

This study investigated the bacterial killing and emergence of resistance of two susceptible *P. aeruginosa* isolates exposed to the expected pharmacokinetics of amikacin in blood and ELF. Following an initial bacterial kill of ≥4-logs within the first 8 h, there was extensive bacterial regrowth for both isolates, with negligible bacterial killing following the first dose. Our results support the current EUCAST recommendation that aminoglycosides may be considered for short-term use in combination with another agent until the antibiotic susceptibilities are confirmed and that aminoglycoside dose optimization may enhance bacterial killing and enhance clinical outcomes (34).

In the current study, achieving a blood and ELF amikacin *f*AUC exposure of approximately >175 (*f*AUC/MIC >21.87) and >366 mg.h/L (*f*AUC/MIC >45.8) respectively, may be sufficient to reduce the bacterial burden of some *P. aeruginosa* isolates to $<10^6$ CFU/mL over 24 h. Such an exposure correlates to an amikacin dose of ≥30 mg/kg or ≥50 mg/kg daily for bloodstream or VAP infections with susceptible *P. aeruginosa* pathogens in patients with

344 normal creatinine clearance (~100 mL/min). However, this threshold may also vary between
345 bacterial isolates as the total bacterial burden within the first 12 h appears to be, in part,
346 mediated by reducing the burden of the susceptible and intermediate-susceptibility bacterial
347 population by achieving the appropriate *f*AUC/MIC and/or *f*C_{max}/MIC. Thereafter, a resistant
348 bacterial population for which amikacin has no effect against may emerge. The emergence of
349 resistance is likely dependent on the relative density of the intermediate/resistant
350 subpopulation(s) in the initial total bacterial inoculum (the mutation frequency) and the
351 propensity for mutations to occur that mediate resistance emergence (35). At the high
352 inoculum used in our study, it was expected based on the mutation frequency that a resistant
353 subpopulation existed, which was subsequently amplified following amikacin administration.
354 This may explain the differences in the identified thresholds for a 1- or 2-log reduction
355 between the susceptible isolates used in this study given that the relative
356 susceptible/intermediate/resistant bacterial populations may differ between isolates. Our
357 results are similar to that previously described against *P. aeruginosa* where a simulated
358 gentamicin plasma C_{max}/MIC ≥36 was unable to suppress bacterial regrowth *in vitro* (9).
359 However, against *Acinetobacter baumannii*, an amikacin C_{max}/MIC of 20 suppressed
360 bacterial regrowth, highlighting the variability in response to aminoglycoside exposure that
361 may be, in part, determined by the inoculum size and pre-existing intermediate/resistant
362 subpopulations.

363

364 Higher ELF amikacin *f*AUC and *f*C_{max} exposures were required to achieve stasis, 1- and 2-
365 logs of bacterial killing over 24 h, which may be related to the delayed and lower *f*C_{max}
366 achieved in the ELF relative to the plasma amikacin concentrations following intravenous
367 administration given the expected pharmacokinetic hysteresis between the bloodstream and
368 ELF. Moreover, there was little bacterial killing against #CTAP40 (MIC 8 mg/L) following a

simulated intravenous 30 mg/kg dose (Figure 2), suggesting that amikacin monotherapy will have little efficacy against higher MIC isolates.

The identified PK/PD targets identified in our study differ to those observed in clinical studies. A previous clinical study in critically ill patients receiving intravenous amikacin demonstrated an increased chance of microbial eradication and clinical cure in patients who achieved a C_{max}/MIC >10 (9). A separate study identified a *f*AUC/MIC ≥150 mg.h/L correlated with faster symptom resolution in patients with nosocomial pneumonia (7, 8). The identified PK/PD ratios from our simulations in this study and clinical studies may be challenging to achieve with doses <30 mg/kg (36, 37). As such, high dose amikacin therapy (>30 mg/kg) may be considered. Limited clinical data exists for such dosing regimens, but doses ≥60 mg/kg have been used as part of salvage therapy in conjunction with renal replacement therapy to minimise the probability of toxicity in a small case series (38). Furthermore, the use of a single dose of amikacin in patients with severe sepsis or septic shock may mitigate the risk of nephrotoxicity, which is unlikely to occur for an aminoglycoside duration <3 days (39). Nevertheless, the use of such high doses would place the patient within an amikacin *f*AUC exposure that has previously been associated with a significant probability of developing nephrotoxicity; however, this is confounded by the different aminoglycosides used and a prolonged treatment duration (40). This approach should be evaluated in a clinical trial to ensure that both the target PK/PD exposures are met and to assess the potential clinical utility of high dose, short duration therapy in terms of patient morbidity and mortality.

Despite the achievement of these targets, resistance may still emerge with amikacin monotherapy. Amikacin resistance was identified for both isolates receiving doses up to 50 mg/kg within 48 h of amikacin initiation. Mutations affecting the ribosomal binding unit ($RplB_{Gly138Leu}$), elongation factors ($FusA_{Leu464Val}$, $Tuf1_{Val21Leu}$) and mucoidal phenotype ($AlgA_{Ala279Asp}$) appear to mediate this resistance, which is consistent with a previous study with tobramycin with similar SNPs within the *rplB* and *fusA* genes that likely inhibit aminoglycoside binding to the 30S ribosomal subunit (41). The relevance of the AlgA mutant is not currently known; however, alteration of alginate production may modify biofilm formation, a known potentiator of antibiotic resistance emergence (42). These mutations were associated with an increased MIC; however, the relative MIC increase was similar following each dosing regimen. Furthermore, a specific mutation was not often consistently identified for all resistant bacterial populations following a specific amikacin dosing regimen. This would suggest that there are either multiple smaller subpopulations that exist, or that alternative resistance mechanisms, such as amikacin efflux exist (43). Nonetheless, given the likely *de novo* emergence of resistance, it is unlikely that subsequent amikacin doses will achieve appreciable further bacterial killing (43). These results would support that notion that amikacin may enhance initial bacterial killing but should be combined with a second agent either empirically or as directed therapy to ensure bacterial eradication and minimise the probability of treatment failure.

Our study is not without limitations. First, the lack of a simulated immune response *in vitro* limits the external validity when applying our results to clinical practice. Nonetheless, as previously discussed, optimising bacterial killing *in vitro* may generalise to optimal clinical outcomes (44). Moreover, our *in vitro* model and subsequent dosing simulations may best represent an immunocompromised patient. Second, only two clinical *P. aeruginosa* isolates

were tested, therefore our results may not generalize to other infecting isolates. Third, the amikacin ELF concentration-time curve is estimated from other aminoglycosides, which may not reflect the exposures achieved for amikacin. This approach may be reasonable given the lack of amikacin-specific data and similar chemical structures between aminoglycosides. Nonetheless, further research detailing the ELF pharmacokinetics of amikacin over a dosing interval are required, thus our results should be considered as hypothesis generating. Fifth, we did not perform WGS on the various phenotypically distinct colonies. This may mean that specific resistance mechanisms may not be appropriately identified if they are present in a sparsely dense bacterial subpopulation. Last, we did not simulate the ELF milieu, which is known to contain mucin, an acidic pH and mucin; factors that are known to impact aminoglycoside-mediated bacterial killing (26, 45-47). The impact of mucin was considered by simulating the estimated unbound amikacin fraction.

Future amikacin intravenous administration may be with the use of a single high dose (≥30 mg/kg) of the antibiotic for patients with either bloodstream infections or VAP from multi-resistant pathogens, such as *P. aeruginosa*, to improve the probability of bacterial eradication. However, this must be balanced with ongoing review of the amikacin doses required for clinical effectiveness against *P. aeruginosa* where doses may result in unacceptable toxicity and combinations with other active anti-pseudomonal agents are preferred. Given the likely low efficacy of bacterial killing in the ELF following intravenous administration, alternate amikacin administration routes, such as nebulized therapy, may be considered. Clinical trials are required to define the optimal dosing regimen of amikacin for difficult to treat infections, such as VAP.

Acknowledgments

Aaron Heffernan would like to acknowledge funding from a Griffith School of Medicine Research Higher degree scholarship. Fekade Sime would like to acknowledge funding from a University of Queensland Post-Doctoral Fellowship. Jason Roberts would like to recognise funding from the Australian National Health and Medical Research Council for a Centre of Research Excellence (APP1099452) and a Practitioner Fellowship (APP1117065). Derek Sarovich is funded by an Advanced Queensland Fellowship (AQRF13016-17RD2). We would like to thank Dr Hanna Sidjabat, Centre for Clinical Research, University of Queensland for kindly providing the isolates used for this study.

References

1. Thaden JT, Park LP, Maskarinec SA, Ruffin F, Fowler Jr VG, van Duin D. 2017. Results from a 13-Year Prospective Cohort Study Show Increased Mortality Associated with Bloodstream Infections Caused by Pseudomonas aeruginosa Compared to Other Bacteria. Antimicrob Agents Chemother **61**:e02671-16.
2. Tumbarello M, De Pascale G, Trecarichi EM, Spanu T, Antonicelli F, Maviglia R, Pennisi MA, Bello G, Antonelli M. 2013. Clinical outcomes of Pseudomonas aeruginosa pneumonia in intensive care unit patients. Intensive Care Med 2013 **39**:682-692.
3. Britt NS, Ritchie DJ, Kollef MH, Burnham CA, Durkin MJ, Hampton NB, Micek ST. 2018. Importance of Site of Infection and Antibiotic Selection in the Treatment of Carbapenem-Resistant Pseudomonas aeruginosa Sepsis. Antimicrob Agents Chemother **62**:e02400-17.
4. Buehrle DJ, Shields RK, Clarke LG, Potoski BA, Clancy CJ, Hong Nguyen M. 2017. Carbapenem-Resistant Pseudomonas aeruginosa Bacteremia: Risk Factors for Mortality and Microbiologic Treatment Failure. Antimicrob Agents Chemother **61**:e01243-16.
5. Sader HS, Farrell DJ, Flamm RK, Jones RN. 2014. Antimicrobial susceptibility of Gram-negative organisms isolated from patients hospitalized in intensive care units in United States and European hospitals (2009-2011). Diagn Microbiol Infect Dis **78**:443-448.
6. Zilberberg MD, Shorr AF, Micek ST, Vazquez-Guillamet C, Kollef MH. 2014. Multi-drug resistance, inappropriate initial antibiotic therapy and mortality in Gram-negative severe sepsis and septic shock: a retrospective cohort study. Crit Care https://doi.org/10.1186/s13054-014-0596-8.
7. Moore RD, Lietman PS, Smith CR. 1987. Clinical response to aminoglycoside therapy: importance of the ratio of peak concentration to minimal inhibitory concentration. J Infect Dis **155**:93-99.
8. Kashuba ADM, Nafziger AN, Drusano GL, Bertino Jr JS. 1999. Optimizing aminoglycoside therapy for nosocomial pneumonia caused by Gram-negative bacteria. Antimicrob Agents Chemother **43**:623-629.
9. Tam VH, Ledesma KR, Vo G, Kabbara S, Lim T, Nikolaou M. 2008. Pharmacodynamic modeling of aminoglycosides against Pseudomonas aeruginosa and Acinetobacter baumannii: identifying dosing regimens to suppress resistance development. Antimicrob Agents Chemother **52**:3987-3993.
10. Shields RK, Clancy CJ, Press EG, Hong Nguyen M. 2016. Aminoglycosides for Treatment of Bacteremia Due to Carbapenem-Resistant Klebsiella pneumoniae. Antimicrob Agents Chemother **60**:3187-3192.
11. Drusano GL, Liu W, Fikes S, Cirz R, Robbins N, Kurhanewicz S, Rodriquez J, Brown D, Baluya D, Louie A. 2014. Interaction of drug- and granulocyte-mediated killing of Pseudomonas aeruginosa in a murine pneumonia model. J Infect Dis **210**:1319-1324.
12. Drusano GL, Fregeau C, Liu W, Brown DL, Louie A. 2010. Impact of burden on granulocyte clearance of bacteria in a mouse thigh infection model. Antimicrob Agents Chemother **54**:4368-4372.
13. Opota O, Croxatto A, Prod'hom G, Greub G. 2015. Blood culture-based diagnosis of bacteraemia: state of the art. Clin Microbiol Infect **21**:313-322.
14. Najmeddin F, Shahrami B, Azadbakht S, Dianatkhah M, Rouini MR, Najafi A, Ahmadi A, Sharifnia H, Mojtahedzadeh M. 2018. Evaluation of Epithelial Lining Fluid Concentration of Amikacin in Critically Ill Patients With Ventilator-Associated Pneumonia. J Intensive Care Med https://doi.org/10.1177/0885066618754784.

15. Wiegand I, Hilpert K, Hancock RE. 2008. Agar and broth dilution methods to determine the minimal inhibitory concentration (MIC) of antimicrobial substances. Nat Protoc **3**:163-175.
16. European Committee for Antimicrobial Susceptibility Testing. 2003. Determination of minimum inhibitory concentrations (MICs) of antibacterial agents by broth dilution. Clin Microbiol Infect https://doi.org/10.1046/j.1469-0691.2003.00790.x.
17. Cadwell J. 2012. The Hollow Fiber Infection Model for Antimicrobial Pharmacodynamics and Pharmacokinetics. Advances in Pharmacoepidemiology & Drug Safety https://doi.org/10.4172/2167-1052.1000S1-007
18. Cadwell J. 2015. The Hollow Fiber Infection Model: Principles and Practice. Advances in Antibiotics and Antibodies **1**:101-106.
19. Romano S, de Gatta MDF, Calvo V, Mendez E, Domínguez-Gil A, Lanao JM. 1998. Influence of clinical diagnosis in the population pharmacokinetics of amikacin in intensive care unit patients. Clinical Drug Investigation **15**:435-444.
20. Brunnemann SR, Segal JL. 1991. Amikacin serum protein binding in spinal-cord injury. Life Sciences **49**:PL1-PL5.
21. Layeux B, Taccone FS, Fagnoul D, Vincent JL, Jacobs F. 2010. Amikacin monotherapy for sepsis caused by panresistant Pseudomonas aeruginosa. Antimicrob Agents Chemother **54**:4939-4941.
22. Panidis D, Markantonis SL, Boutzouka M, Karatzas, S, Baltopoulos G. 2005. Penetration of gentamicin into the alveolar lining fluid of critically ill patients with ventilator-associated pneumonia. Chest **128**:545-552.
23. Boselli E, Breilh D, Djabarouti S, Guillaume C, Rimmelé T, Gordien J, Xuereb F, Saux M, Allaouchiche B. 2007. Reliability of mini-bronchoalveolar lavage for the measurement of epithelial lining fluid concentrations of tobramycin in critically ill patients. Intensive Care Med **33**:1519-1523.
24. Bowker KE, Noel AR, Tomaselli S, Attwood M, MacGowan AP. 2018. Pharmacodynamics of inhaled amikacin (BAY 41-6551) studied in an in vitro pharmacokinetic model of infection. J Antimicrob Chemother **73**:1305-1313.
25. Stass H, Willmann S, Windl T. 2014. Risk assessment for amikacin inhale in ICU patients using whole-body physiologically based PK-models, abstr P-926, p 232. 43rd Critical Care Congress. Society of Critical Care Medicine, San Francicso, CA.
26. Huang JX, Blaskovich MA, Pelingon R, Ramu S, Kavanagh A, Elliott AG, Butler MS, Montgomery AB, Cooper MA. 2015. Mucin Binding Reduces Colistin Antimicrobial Activity. Antimicrob Agents Chemother **59**:5925-5931.
27. Sarovich D. 2017. MGAP---Microbial-Genome-Assembler-Pipeline. Zenodo. https://doi.org/10.5281/zenodo.825368
28. Seemann T. 2014. Prokka: rapid prokaryotic genome annotation. Bioinformatics 2014.**15** 30:2068-2069.
29. Sarovich DS, Price EP. 2014. SPANDx: a genomics pipeline for comparative analysis of large haploid whole genome re-sequencing datasets. BMC Res Notes https://doi.org/10.1186/1756-0500-7-618.
30. McKenna A, Hanna M, Banks E, Sivachenko A, Cibulskis K, Kernytsky A, Garimella K, Altshuler D, Gabriel S, Daly M, DePristo MA. 2010. The Genome Analysis Toolkit: a MapReduce framework for analyzing next-generation DNA sequencing data. Genome Res **20**:1297-1303.
31. Aziz A, Currie BJ, Mayo M, Sarovich DS, Price P. 2020. Comparative genomics confirms a rare melioidosis human-to-human transmission event and reveals incorrect phylogenomic reconstruction due to polyclonality. Microb Genom https://doi.org/10.1099/mgen.0.000326.

566 32. Neely MN, van Guilder MG, Yamada WM, Schumitzky A, Jelliffe RW. 2012.
567 Accurate detection of outliers and subpopulations with Pmetrics, a nonparametric and
568 parametric pharmacometric modeling and simulation package for R. Ther Drug Monit
569 **34**:467-476.
570 33. Gumbo T, Louie A, Deziel MR, Parsons LM, Salfinger M, Drusano GL. 2004.
571 Selection of a moxifloxacin dose that suppresses drug resistance in Mycobacterium
572 tuberculosis, by use of an in vitro pharmacodynamic infection model and mathematical
573 modeling. J Infect Dis **190**:1642-1651.
574 34. European Committee for Antimicrobial Susceptibility Testing. 2020. Guidance
575 document on implementation and use of the revised aminoglycoside breakpoints.
576 35. Martinez JL, Baquero F. 2000. Mutation frequencies and antibiotic resistance.
577 Antimicrob Agents Chemother **44**:1771-1777.
578 36. Roger C, Nucci B, Louart B, Friggeri A, Knani H, Evrard A, Lavigne J, Allaouchiche
579 B, Lefrant J, Roberts JA, Muller L. 2016. Impact of 30 mg/kg amikacin and 8 mg/kg
580 gentamicin on serum concentrations in critically ill patients with severe sepsis. J Antimicrob
581 Chemother **71**:208-212.
582 37. Roger C, Nucci B, Molinari N, Bastide S, Saissi G, Pradel G, Barbar S, Aubert C,
583 Lloret S, Elotmani L, Polge A, Lefrant J, Roberts JA, Muller L. 2015. Standard dosing of
584 amikacin and gentamicin in critically ill patients results in variable and subtherapeutic
585 concentrations. Int J Antimicrob Agents **46**:21-27.
586 38. Brasseur A, Hites M, Roisin S, Cotton F, Vincent J, DeBacker D, Jacobs F, Taccone
587 FS. 2016. A high-dose aminoglycoside regimen combined with renal replacement therapy for
588 the treatment of MDR pathogens: a proof-of-concept study. J Antimicrob Chemother
589 **71**:1386-1394.
590 39. Picard W, Bazin F, Clouzeau B, Bui H, Soulat M, Guilhon E, Vargas F, Hilbert G,
591 Bouchet S, Gruson D, Moore N, Boyer A 2014. Propensity-based study of aminoglycoside
592 nephrotoxicity in patients with severe sepsis or septic shock. Antimicrob Agents Chemother
593 **58**:7468-7474.
594 40. Drusano GL, Ambrose PG, Bhavnani SM, Bertino JS, Nafziger AN, Louie A. 2007.
595 Back to the future: using aminoglycosides again and how to dose them optimally. Clin Infect
596 Dis **45**:753-760.
597 41. Feng Y, Jonker MJ, Moustakas I, Brul S, Ter Kuile BH. 2016. Dynamics of
598 Mutations during Development of Resistance by Pseudomonas aeruginosa against Five
599 Antibiotics. Antimicrob Agents Chemother **60**:4229-4236.
600 42. Bagge N, Schuster M, Hentzer M, Ciofu O, Givskov M, Greenberg EP, Høiby N.
601 2004. Biofilms Exposed to Imipenem Exhibit Changes in Global Gene Expression and β-
602 Lactamase and Alginate Production. Antimicrob Agents Chemother **48**:1175-1187.
603 43. Barclay ML, Begg EJ, Chambers ST, Thornley PE, Pattemore PK, Grimwood K.
604 1996. Adaptive resistance to tobramycin in Pseudomonas aeruginosa lung infection in cystic
605 fibrosis. J Antimicrob Chemother **37**: 1155-1164.
606 44. Gumbo T, Pasipanodya JG, Romero K, Hanna D, Nuermberger E. 2015. Forecasting
607 Accuracy of the Hollow Fiber Model of Tuberculosis for Clinical Therapeutic Outcomes.
608 Clin Infect Dis **61**:S25-S31.
609 45. Bataillon V, Lhermitte M, Lafitte JJ, Pommery J, Roussel P. 1992. The binding of
610 amikacin to macromolecules from the sputum of patients suffering from respiratory diseases.
611 J Antimicrob Chemother **29**:499-508.
612 46. van 't Veen A, Mouton JW, Gommers D, Kluytmans JA, Dekkers P, Lachmann B.
613 1995. Influence of pulmonary surfactant on in vitro bactericidal activities of amoxicillin,
614 ceftazidime, and tobramycin. Antimicrob Agents Chemother **39**:329-333.

47. Bodem CR, Lampton LM, Miller DP, Tarka EF, Everett ED. 1983. Endobronchial pH. Relevance of aminoglycoside activity in gram-negative bacillary pneumonia. Am Rev Resp Dis **127**:39-41.

Table 1: *Pseudomonas aeruginosa* amikacin minimum inhibitory concentrations from isolates grown on amikacin-containing (4x baseline MIC) cation adjusted Mueller-Hinton agar after the 7-day course

Isolate	Amikacin Dose	MIC (mg/L)
#CTAP23	15 mg/kg	32
	25 mg/kg	32
	50 mg/kg	64
	30 mg/kg (ELF)	16
#CTAP40	15 mg/kg	64
	25 mg/kg	128
	50 mg/kg	128
	30 mg/kg (ELF)	64

Table 2: Variation identified in comparison to the initial starting strain in the #CTAP23 and #CTAP40 lineages. Percentages reflect the prevalence of the mutation within the population.

	*fusA*_2 1390	*rplB* 413	*rplB* 412	*algA*_1 836	*tuf1*_1
#CTAP23 Baseline	0%	0%	0%		
#CTAP23 15 mg/kg	0%	2%	2%		
#CTAP23 25 mg/kg	57%	4%	4%		
#CTAP23 50 mg/kg	0%	100%	100%		
#CTAP40 Baseline				13%	0%
#CTAP40 15 mg/kg				69%	55%
#CTAP40 25 mg/kg				98%	19%
#CTAP40 50 mg/kg				60%	0%

690 Table 3: Pharmacodynamic model parameter estimates

Parameter	Abbreviation	#CTAP23	#CTAP40
		Mean (SD)	Mean (SD)
Susceptible Growth Rate constant (log10 CFU/mL/h)	Kgs	1.31 (0.11)	1.08 (0.20)
Intermediate Growth Rate constant (log10 CFU/mL/h)	Kgr	0.40 (0.13)	0.60 (0.26)
Resistant Growth Rate constant (log10 CFU/mL/h)	Kgrr	0.69 (0.11)	0.55 (0.13)
Central compartment HFIM volume (L)	Vc	0.32 (0.01)	0.26 (0.05)
Amikacin clearance (L/h)	Cl	0.03 (0.00)	0.03 (0.00)
Susceptible Killing Rate Constant (log10 CFU/mL/h)	Emaxs	5.34 (1.50)	4.00 (3.01)
Intermediate Killing Rate Constant (log10 CFU/mL/h)	Emaxr	9.43 (3.19)	11.20 (2.10)
Amikacin concentration causing 50% Emaxs (mg/L)	EC50s	11.61 (3.49)	11.10 (2.53)
Amikacin concentration causing 50% Emaxr (mg/L)	EC50r	244.09 (149.73)	349.63 (79.19)
Susceptible Hill Coefficient	Hs	6.00 (4.27)	11.04 (5.80)
Resistant Hill Coefficient	Hr	3.42 (2.47)	7.71 (2.61)
Intermediate population initial condition (CFU/mL)	ICRe	211.05 (119.12)	320.48 (50.57)
Resistant population initial condition (CFU/mL)	ICRRe	29.46 (48.23)	25.81 (16.70)
Maximum substrate consumption	Qmax	0.81 (0.18)	0.59 (0.29)
Maximum available substrate	Substrate	3.33x1010 (2.22x1010)	4.92x1010 (2.75x1010)
Substrate concentration causing 50% Qmax	Qs	8.15x105 (9.61x104)	5.3x105 (1.69x105)
Death rate constant susceptible population	Kds	0.25 (0.15)	0.05 (0.04)
Death rate constant intermediate population	Kdi	0.24 (0.18)	0.02 (0.03)
Death rate constant resistant population	Kdr	0.03 (0.02)	0.11 (0.32)

691

692 The mean and standard deviation (SD) for each parameter and isolate were determined using
693 the average and bootstrapped estimates respectively of the posterior model estimates for each
694 dosing regimen.

695

696

697

698

699

700

701

702

703

Table 4: Pharmacokinetic/Pharmacodynamic exposures required for bacterial stasis, 1-log, and 2-log reduction in the total bacterial burden over 24 h.

Isolate	Infection Site	Exposure Target	Stasis	1-log kill	2-log kill
#CTAP40	Blood	*f*AUC	108.81	124.70	174.95
		*f*AUC/MIC	13.60	15.59	21.87
		*f*Cmax	24.73	25.86	27.15
		*f*Cmax/MIC	3.09	3.23	3.39
	ELF	*f*AUC	328.21	342.69	366.42
		*f*AUC/MIC	41.03	42.84	45.80
		*f*Cmax	42.41	47.47	54.17
		*f*Cmax/MIC	5.30	5.93	6.77
#CTAP23	Blood	*f*AUC	117.54	-	-
		*f*AUC/MIC	58.77		
		*f*Cmax	26.41	-	-
		*f*Cmax/MIC	13.21		
	ELF	*f*AUC	342.92	688.54	688.82
		*f*AUC/MIC	171.46	344.27	344.1
		*f*Cmax	47.04	42.40	47.81
		*f*Cmax/MIC	23.52	21.20	23.91

734 Table 5: Probability of achieving either bacterial stasis, a 1-log reduction, or 2-log reduction
735 in the total bacterial population within 24 h of commencing intravenous amikacin

Isolate	Infection Site	Dose	Renal Function (mL/min)	Stasis	1-log kill	2-log kill
#CTAP40	Blood	15 mg/kg	60	1	1	1
		30 mg/kg	60	1	1	1
		50 mg/kg	60	1	1	1
		15 mg/kg	100	1	0.99	0.89
		30 mg/kg	100	1	1	1
		50 mg/kg	100	1	1	1
		15 mg/kg	140	0.90	0.52	0.16
		30 mg/kg	140	1	1	1
		50 mg/kg	140	1	1	1
	ELF	15 mg/kg	60	0	0	0
		30 mg/kg	60	0.93	0.44	0.03
		50 mg/kg	60	1	1	1
		15 mg/kg	100	0	0	0
		30 mg/kg	100	0.41	0.03	0
		50 mg/kg	100	1	1	1
		15 mg/kg	140	0	0	0
		30 mg/kg	140	0.02	0	0
		50 mg/kg	140	1	1	1
#CTAP23	Blood	15 mg/kg	60	1	0	0
		30 mg/kg	60	1	0	0
		50 mg/kg	60	1	0	0
		15 mg/kg	100	0.99	0	0
		30 mg/kg	100	1	0	0
		50 mg/kg	100	1	0	0
		15 mg/kg	140	0.69	0	0
		30 mg/kg	140	1	0	0
		50 mg/kg	140	1	0	0
	ELF	15 mg/kg	60	0	0	0
		30 mg/kg	60	0.57	0	0
		50 mg/kg	60	1	0	0
		15 mg/kg	100	0	0	0
		30 mg/kg	100	0.06	0	0
		50 mg/kg	100	1	0	0
		15 mg/kg	140	0	0	0
		30 mg/kg	140	0	0	0
		50 mg/kg	140	1	0	0

736

737

738

Antimicrobial Agents and Chemotherapy

739

740 Figure 1: Total bacterial population for different amikacin dosing regimen in either blood or
741 the epithelial lining fluid (ELF) over 168 h. A; #CTAP23 and B; #CTAP40.

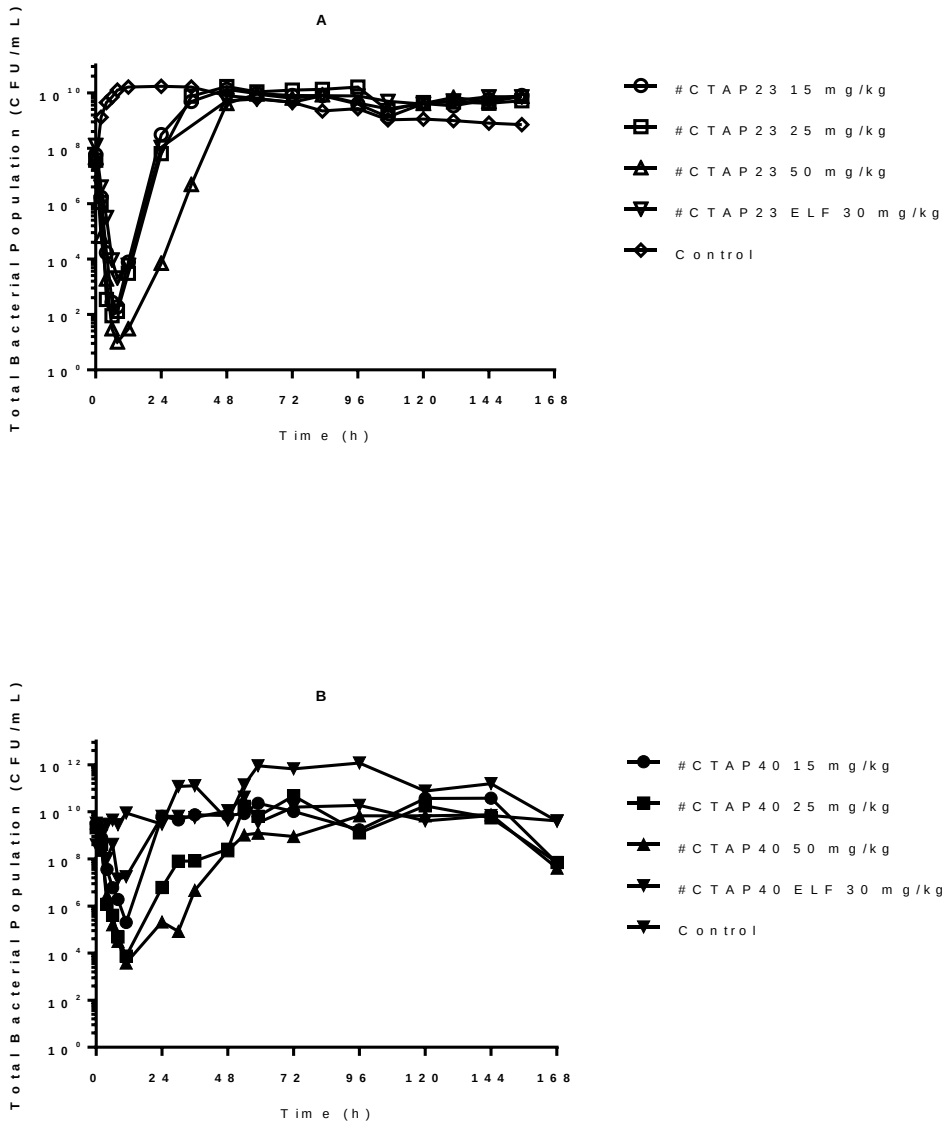

742
743

744

745

746

747

748

749 Figure 2: Total bacterial population (filled lines) and resistant population (dashed lines) for
750 #CTAP23 and #CTAP40 in blood (amikacin dosing regimens 15, 25 and 50 mg/kg) and
751 epithelial lining fluid (amikacin dosing regimen 30 mg/kg).

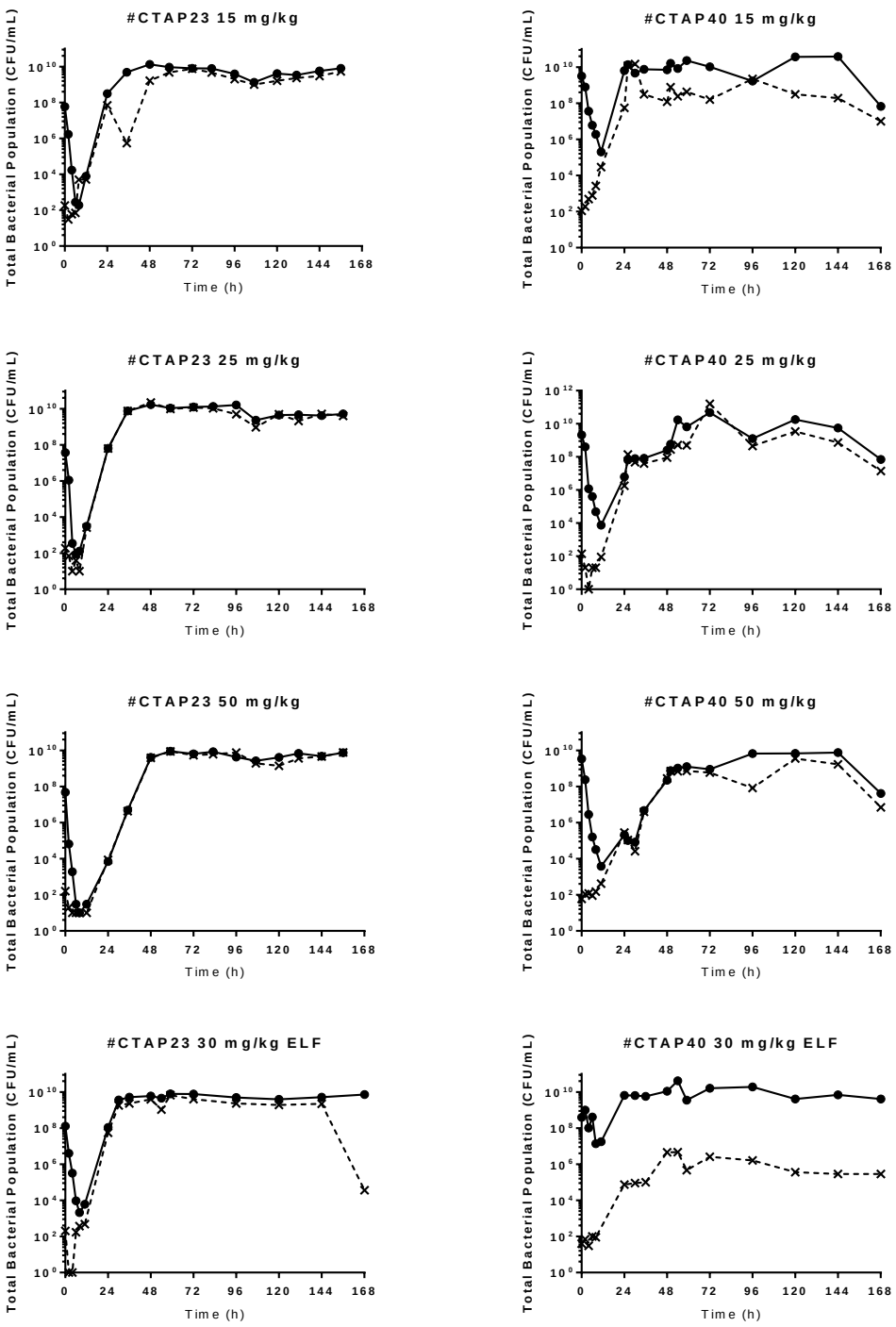

752
753

754 Figure 3: Pharmacokinetic/Pharmacodynamic model observed-predicted fit for isolate
755 #CTAP23. A; amikacin pharmacokinetic data. B and C; Total bacterial population observed

vs. predicted values for the population and posterior estimates respectively. D and E; Resistant bacterial population observed vs. predicated values for the population and posterior estimates respectively. Circles #CTAP 23 15 mg/kg; triangles #CTAP23 25 mg/kg; squares #CTAP23 50 mg/kg; hexagons #CTAP23 ELF Exposure; diamonds #CTAP23 Control

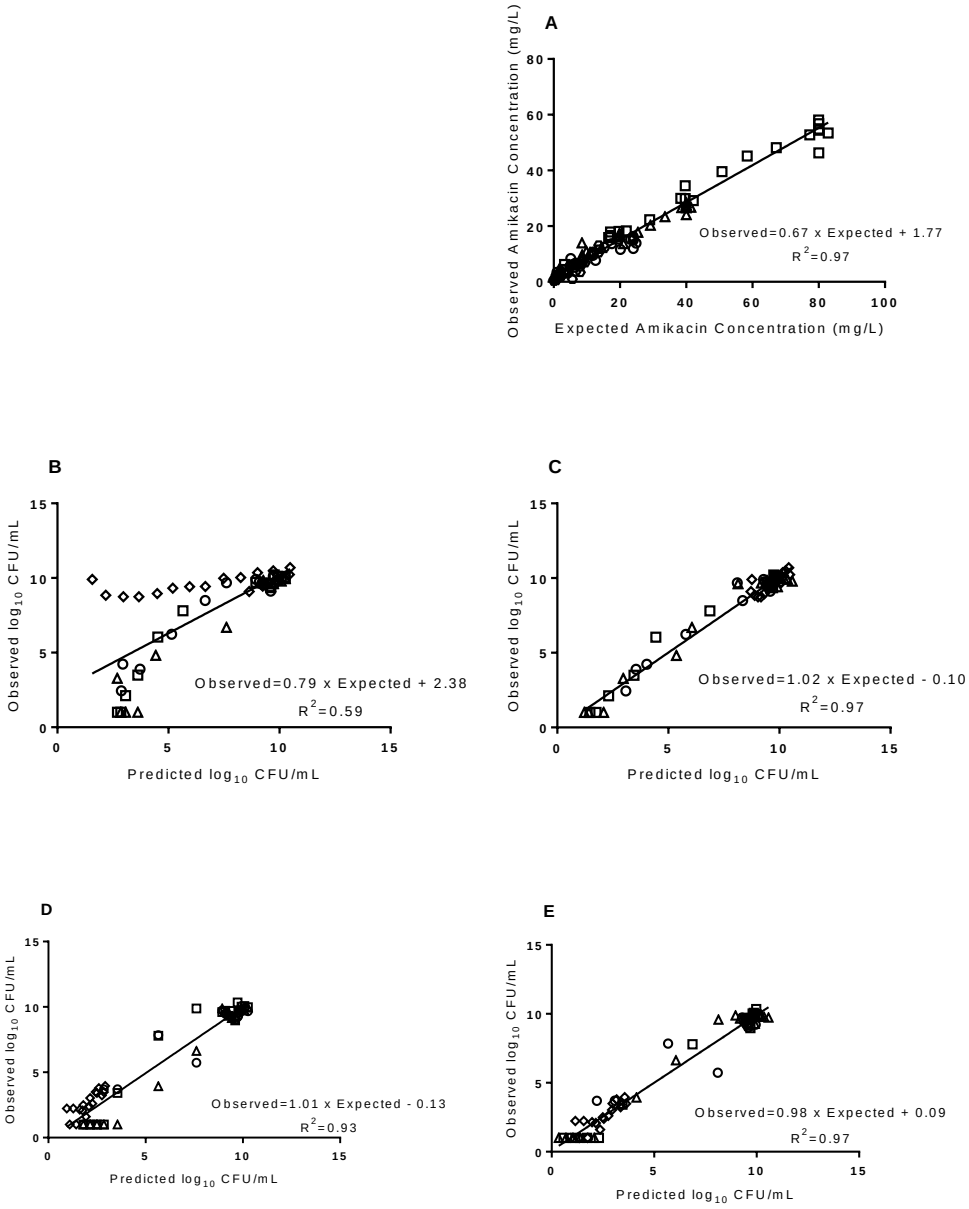

Figure 4: Pharmacokinetic/Pharmacodynamic model observed-predicted fit for isolate #CTAP40. A; amikacin pharmacokinetic data. B and C; Total bacterial population observed

vs. predicted values for the population and posterior estimates respectively. D and E; Resistant bacterial population observed vs. predicated values for the population and posterior estimates respectively. Circles #CTAP 23 15 mg/kg; triangles #CTAP23 25 mg/kg; squares #CTAP23 50 mg/kg; hexagons #CTAP23 ELF Exposure; diamonds #CTAP23 Control